Novel Photodetectors Using Metal-Oxide-Silicon Tunneling Structures

B.-C. Hsu, W. T. Liu, C.-H. Lin and C. W. Liu[a]
Department of Electrical Engineering, National Taiwan University, Taipei, Taiwan
Tel: 886-2-23635251 ext. 515; Fax: 886-2-23638247 E-mail: chee@cc.ee.ntu.edu.tw
[a] also with Graduate Institute of Electronics Engineering

Abstract — Metal/oxide/Si structures with ultrathin gate oxide are utilized as photodetectors. At inversion gate bias, the dark current and photocurrent are determined by both the minority carrier generation rate in the deep depletion region and the electrons tunneling from the gate electrode to n-type Si in a PMOS detector, while only the former component is significant in the NMOS photodetector. The electron tunneling current dominates the photocurrent at sufficiently large negative gate voltage, and the sensitivity of PMOS detectors is, therefore, enhanced by approximately one order of magnitude, as compared to NMOS detectors.

I. Introduction

Various semiconductor photodetectors and image sensors have been fabricated and studied such as charge coupled devices, photodiodes (p-i-n, Schottky, heterojunction, avalanche), and capacitive photodetectors [1]. The significant tunneling gate current of metal-oxide-silicon (MOS) diodes with ultrathin gate oxide can be applied to add new functions of MOS devices. Both NMOS [2] and PMOS [3] light emitting diodes have been demonstrated. The NMOS photodetector have been also demonstrated as biased in the deep depletion region [4]. In this work, we report the results of PMOS photodetector and enhanced sensitivity is observed. The fully CMOS-compatible light sources and detectors make it possible to have optoelectronic applications using a CMOS process.

II. Device Fabrication

The ultrathin gate oxide of the MOS diode is grown by rapid thermal oxidation on 1-5 Ω-cm n-type wafer at 900~1000°C. The gas flows are 500 sccm nitrogen and 500 sccm oxygen at reduced pressure. The Al is used as the gate electrodes of PMOS diodes with the circular areas defined by photolithography. The device structure is shown in the inset of Fig. 1.

III. Device Operation

Fig. 1 is the I-V curves of an NMOS photodetector. Fig. 2 is the I-V curves of a PMOS detector with an area of 3.2×10^{-4} cm^2. The photocurrent was excited by metal halide lamp with a spectrum similar to sun. The dark and photocurrents are relatively constant in the log scale at sufficiently large inversion gate bias for both devices. For the photocurrent of PMOS, the stepwise I-V curves indicate that there are two components in the photocurrents. Under the same light exposure, the current magnitude at the first plateau of the I-V curves of PMOS detectors (gate

voltage = -0.8 V) is similar to that of a NMOS photodiode with similar substrate resistivity (Fig.3). The photocurrent of a NMOS detector is determined by the minority (electron) generation rate in the deep depletion region, since the tunneling rate through the ultrathin oxide is sufficiently large at large gate bias [4]. Therefore, the first plateau of I-V curves of PMOS detector should originate from the minority (hole) generation rate in the deep depletion region. Both NMOS and PMOS photodetectors have the same magnitude of photocurrent at the first plateau under the same intensity of light exposure, since the electron generation rate in NMOS and the hole generation rate in PMOS are the same at the same light intensity. The hole concentration at Si/oxide interface of a PMOS detector is balanced by the photo-generation rate and the tunneling rate through the oxide. As negative gate bias continues to increase, the hole concentration at oxide/Si interface increases slowly, and oxide voltage also increases very slightly (soft pinning) [4]. The calculated oxide voltage vs the applied gate voltage of PMOS device under different light exposure is given in Fig. 4. The calculation model is described in Fig. 5, and the parameter used for holes are $A=1x10^{-5}\ s^{-1}$, $C=6.325x10^{6}\ V^{-0.5}cm^{-1}$, $t_{ox}=2.7$ nm, $\phi_O=4.5$ eV, and $N_A=5x10^{15}\ cm^{-3}$. The oxide voltage increases with light exposure intensity, but still constitutes small fraction of the gate voltage.

The oxide voltage causes the direct tunneling of electrons from the Al gate to n-type Si in PMOS detectors. This direct tunneling electron current forms the second plateau in the I-V curves in a PMOS detector, which is approximately one order magnitude larger than the photo-generated hole current at the first plateau (Fig. 3). Most gate voltage drops on Si and a deep depletion region is formed. The soft pinning of oxide voltage at large negative gate bias restricts the further increase of the direct tunneling electron current, which is strongly dependent on oxide voltage, and the photocurrent is relatively constant after some gate bias. Fig. 6 illustrates these two mechanisms. Fig. 7 is the current transport mechanism of NMOS detector. The NMOS photodetector with Al gate has a barrier height of ~5.6 eV for holes tunneling from Al to p-Si substrate, which is much larger than electron barrier height (~ 3.2 eV) in PMOS. This leads to a negligible direct tunneling hole current in a NMOS detector. The second plateau, therefore, is not observed in the I-V curve of NMOS detectors [4].

By comparing photocurrents in NMOS detectors with Al and transparent ITO (indium tin oxide) electrodes, the edge absorption of light around the non-transparent Al electrode is approximately 5% of the absorption of the ITO gate. The measured external quantum efficiency of Al gate PMOS is 4% if the first plateau current is used as the photo signal, which is similar to the efficiency of Al gate NMOS. However, the efficiency of the PMOS detector can be as high as 40% if the second plateau is used as the photo signal. For current devices, no efficiency-enhanced structures such as grid gate electrodes (semi-transparent), transparent gate electrodes, and anti-reflection coating are used, but the optimization is under progress. The measured responsivity in the infrared region of the PMOS detector is given in Fig. 8. This PMOS photodetector has a cut-off wavelength at 1.2 μm.

IV. CONCLUSION

Photodetectors using both the PMOS and NMOS tunneling structures are demonstrated. The direct tunneling electron current from Al electrode to n-type silicon is the main component of the photocurrent in PMOS, which is one order of magnitude larger than minority generation current in the deep depletion region. The two plateaus in the I-V curves of the photocurrent are the signatures of these two mechanisms. The direct tunneling hole current in the NMOS is very small, and only the minority (electron) generation current forms the photocurrent. As a result, the sensitivity of a PMOS detector is much larger than that of a NMOS detector.

REFERENCES

[1] B. C. Paul, M. Satyam, and A. Selvarajan, "A Novel Method of Optical Detection Using a Capacitive Device," *IEEE Transactions on Electron Devices*, vol. 46, pp. 324-328, 1999.

[2] C. W. Liu, M. H. Lee, M.-J. Chen, C.-F. Lin and M. Y. Chern, "Roughness -Enhanced Electroluminescence from Metal Oxide Silicon Tunneling Diodes," *IEEE Electron Device Lett.*, vol. 21, pp. 601-603, 2000.

[3] C. W. Liu, M. H. Lee, M.-J. Chen, C.-F. Lin and I. C. Lin, "Room-temperature electroluminescence from electron-hole plasmas in the metal oxide silicon tunneling diodes," *Appl. Phys. Lett.*, vol. 76, pp. 1516-1518, 2000.

[4] C. W. Liu, W. T. Liu, M. H. Lee, W. S. Kuo and B. C. Hsu, "A novel photodetector using MOS tunneling structures," *IEEE Electron Dev. Lett.*, vol. 21, pp. 307-309, 2000.

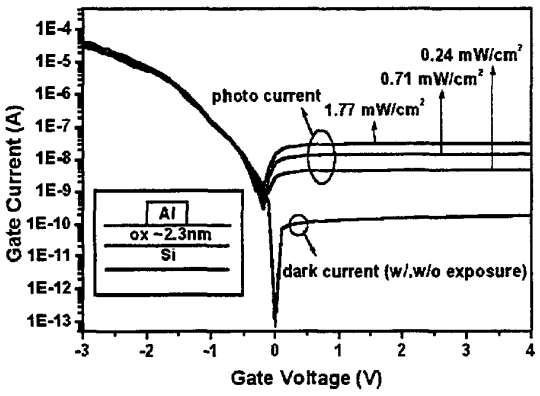

Fig. 1 The dark current and photocurrent of a NMOS tunneling photodetector. The inset is the device structure.

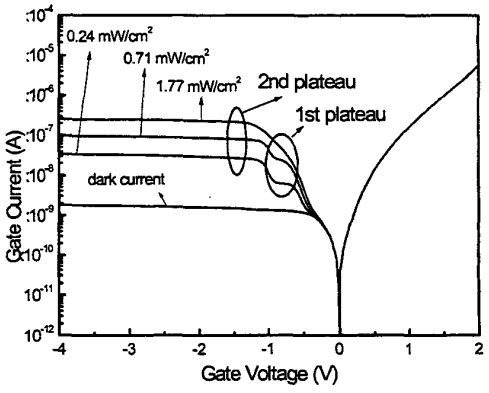

Fig. 2 The dark and photocurrent of a PMOS tunneling photodetector.

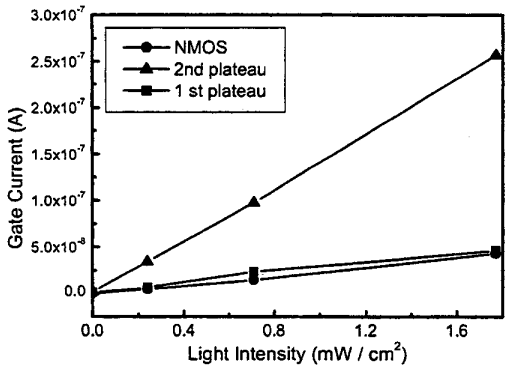

Fig. 3 The photocurrent vs light intensity at the first plateau and the second plateau of I-V curves of a PMOS photodetector as well as for NMOS. photodetectors.

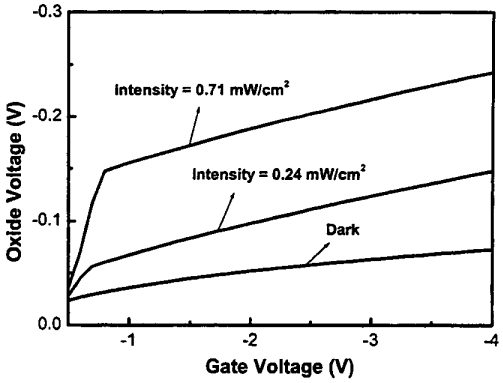

Fig. 4 The oxide voltage vs gate voltage under different light intensity.

$$V_{ox} = -\frac{Q_I + Q_B}{C_{ox}}$$

$$I_s = \Gamma \cdot Q_I$$

$$Q_B = \sqrt{qN_A \kappa_{Si} \varepsilon_0 (2\varphi_s)}$$

$$V_G = V_{FB} + V_{OX} + \varphi_S$$

$$\Gamma = A \cdot \exp\left\{-C\frac{t_{ox}}{V_{ox}}\left[\phi_0^{3/2} - (\phi_0 - V_{OX})^{3/2}\right]\right\}$$

Fig. 5. Equations relevant for the simulated model. Γ is the transmission rate, estimated by WKB methods in the direct tunneling region.

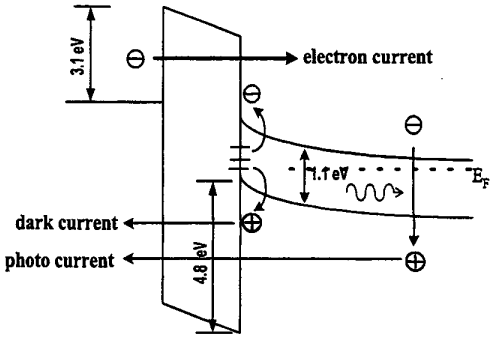

Fig. 6 A schematic diagram of photocurrent mechanisms for a PMOS photodetector.

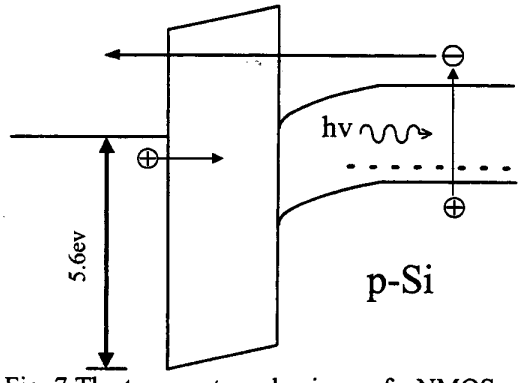

Fig. 7 The transport mechanisms of a NMOS photodetector.

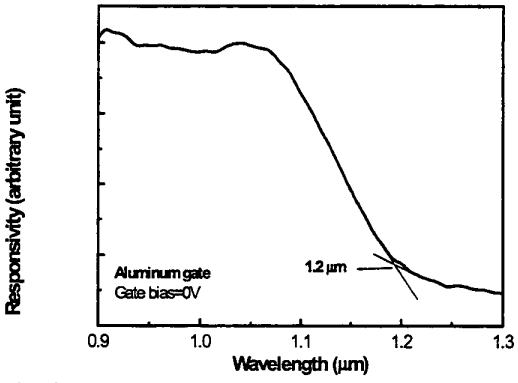

Fig. 8 The measured responsivity of the PMOS Photodetector.